We are IntechOpen,
the world's leading publisher of
Open Access books
Built by scientists, for scientists

4,800

Open access books available

122,000

International authors and editors

135M

Downloads

Our authors are among the

154

Countries delivered to

TOP 1%

most cited scientists

12.2%

Contributors from top 500 universities

CLARIVATE ANALYTICS

BOOK CITATION INDEX

INDEXED

WEB OF SCIENCE™

Selection of our books indexed in the Book Citation Index
in Web of Science™ Core Collection (BKCI)

Interested in publishing with us?
Contact book.department@intechopen.com

Numbers displayed above are based on latest data collected.
For more information visit www.intechopen.com

Direct Power Control for Switched Reluctance Generator in Wind Energy

Tárcio A. dos S. Barros, Alfeu J. Sguarezi Filho and
Ernesto Ruppert Filho

Additional information is available at the end of the chapter

1. Introduction

Wind energy is one of the renewable energy must used actually. It is the kinetic energy contained in moving air masses. Its use occurs through the conversion of kinetic energy translation in kinetic energy of rotation with the use of wind turbines to produce electricity. To ensure the best exploration of wind energy is necessary the use of generators that take of this energy form more efficient in variable speed systems. The electrical induction machines and synchronous generators are widely used in wind turbines. The switched reluctance generator has been studied and pointed as a good solution for applications for wind generation systems of up to 500kW [1].

The switched reluctance generator (SRG) has as main characteristics: mechanical robustness, high starting torque,high performance and low cost. The SRG can operate at variable speeds and its operating range is broader than synchronous and induction generators. Some works that study the behavior of the SRG in case of variable speed are presented in [2–4]. In these studies, the control systems used for power control of SRG are controls that utilize pulse width modulation control and a current loop, but the use of these controllers has shown that their performances are not satisfactory due to switching losses and consequently decrease of efficiency in operations with varying speeds of SRG.

An alternative for the power control of electrical machine is the direct power control (DPC). This technique allows to control directly the power without the use current loops or torque and flux loops and it is applied satisfactory in DFIG and inverters [5] .

In this work is performed a control method of the switched reluctance generator through simulation techniques using mathematical models of the studied system. A wind power generation system with the SRG connected to the grid was performed based on control of

two separate converters. The control of the converter connected to the SRG regulates the extraction of electrical power to be generated and the control of the converter connected to the grid is responsible for regulate the transmission of the generated energy to the grid. A direct power control was developed to control the power generated by SRG. Unlike most of SRG control schemes found in the literature in which the power of the SRG is indirectly controlled by a current loop, the direct control of power acts directly on the power generated by SRG. The energy generated by SRG is sent to the grid by a voltage source converter, which also controls the active power delivered to the grid.

2. Wind Energy Systems

From 1998 to 2008 the growth of wind power installed in the world was approximately 30% and in the last three years the value of installed wind power kept in the mean 45GW, with a total current value of 237.7 GW of installed power in the world. China has the largest installed wind power value (about 62.3 GW) followed U.S. (46.9 GW) and Germany (29.06 GW) [1].

The electrical machine widely used as a generator in wind power generation systems are the induction and synchronous [6, 7]. These generators can operate with variable speed depending on the use of electronic converters for the processing energy of generators. A machine that can be used in wind power generation systems is the switched reluctance machine [8, 9].

A schematic diagram of wind power generation system connected to the grid using the SRG is shown in Figure 1. This system is based on the control generation of two separate converters. The converter connected to the SRG regulates the maximum extraction of electric power according to the profile of wind system.
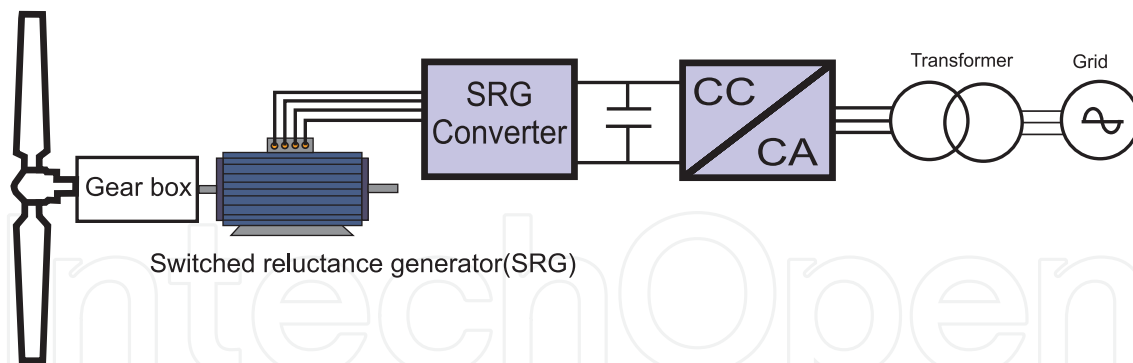

Figure 1. Structure of cascade converters for wind generation using the SRG.

In the literature were found articles that discuss the connection of SRG and the grid in wind power generation systems with variable speed. In [4] the authors used two strategies to control output power of a SRG 8/6. These experiments demonstrated a high efficiency of the system to a wide range of variation of speed. However, the PWM control used is contested by [10] for its hardware complexity for variable speed situations in a wide range of speeds. The converter used in [4] to drive the SRG uses a converter *buck* to magnetize the phases of the machine. This increases the cost and complexity of the converter.

In [2] was developed a system to control the power generated by the SRG using a hysteresis control. It was observed a satisfactory result just to low speed operation. In [11] has been proposed a control system where the power sent to the grid is controlled directly by the inverter connected to the grid. It was observed that this form of control has slow response and poor performance in situations of high speed variations.

A system that consists in controlling the power generated by a SRG 6/4 connected to a DC network has been proposed in [12]. The converter used requires a converter *buck-boost* voltage to regulate the magnetization of the SRG.

An alternative analyzed in studies in literature relates to the development of controllers to connect the SRG directly to the load to be fed through the converter SRG. In [13, 14] controls were performed using fuzzy logic to keep the generated voltage constant. Other controls using optimization of switching angle of of SRG were performed in [15, 16], but require high processing power and storage tables.

2.1. Mechanical power extracted from the wind

To use the energy contained in wind is necessary to have a continuous and fairly strong wind flux. The modern wind turbines are designed to achieve the maximum power in wind speeds in the order of 10 to 15m/s. The energy available for a wind turbine is the kinetic energy associated with a column of air that moves at a constant uniform speed. The mathematical model allows to calculate the aerodynamic torque mechanical value or mechanical power applied to the shaft of the electric generator from the information of the wind speed and position value of the step angle of the turbines. The model also depends on the type of the turbine to be represented as having the characteristics of vertical or horizontal axis, number of blades, blade angle control, and regardless of the type of electrical generator chosen or the type of control of converters. Accordingly, this allows it to be studied regardless of the types of electrical generators. The mechanical power in steady state can be extracted from the wind is shown in Equation 1 [17–19].

$$P_m = \frac{1}{2}\rho A v^3 C_p\left(\psi, \beta_t\right) \qquad (1)$$

Since P_m mechanical power of the turbine, ρ density of air, A area swept by the turbine blades, v wind speed and C_P coefficient of performance, ψ a linear relation $\dfrac{\omega_r\, R_t}{V}$, R_t the radius of the turbine and β_t pitch angle of the vanes of the turbine. The power coefficient of C_P indicates the efficiency with which the wind turbine transforms the kinetic energy contained in wind into mechanical energy rotating. The power ratio depends on the linear relationship between the wind speed and the speed of the propeller tip psi and the propeller pitch angle β_t.

In expression (1) it appears that the mechanical power (P_m) generated by wind power directly depends on the power coefficient C_P. On the other hand, considering the pitch angle of the vanes fixed to zero, the power coefficient depends exclusively on the relationship between the velocity and the linear speed of the tip of the helix, therefore the mechanical power produced by a wind turbine is varied according to their operating speed. For each value

of the wind speed is a region in which the rotor speed maximizes the mechanical power generated. Therefore, for wind speeds below rated speed operation with variable speed rotor increases efficiency in power generation [18, 19]. The profile of optimizing the efficiency of the power generated for variable speeds can be expressed by:

$$P_{opt} = k_{opt} w_r^3 \tag{2}$$

Where P_{opt} is the optimum power and k_{opt} depends of aerodynamics of the helix, gear box and parameters of the wind turbine.

3. Structure and operation principle of the switched reluctance machine

The switched reluctance machine (SRM) is a primitive conception, and its basic concept of operation has been established for around 1838. However, only with the development of the power electronics has become possible to use this machine operating system for applications requiring variable speed [20].

3.1. Basic structure

SRM is a double salient (in rotor and in stator) having field coils in stator as the DC motor and does not have coils or magnets in the rotor. The rotor is composed of ferromagnetic material with salient regularly. Figure 2 there is a MRV 8/6 (number of stator poles/rotor poles number). Other possibilities existing construction are 6/4, 10/4, 12/8 and 12/10, among other configurations.

The operation principle of the MRV as motor is based on the principle of minimum reluctance, ie, when the winding on a stator pole pair is energized, the poles of the rotor are attracted to a position that represents the minimum reluctance (axes aligned), generating a torque on the rotor. while two rotor poles are aligned with the stator poles other poles are out of alignment rotor. These other stator poles are driven bringing the rotor poles into alignment. By the sequential switching of the stator windings, there is production of electromagnetic torque and the rotor rotates [10].
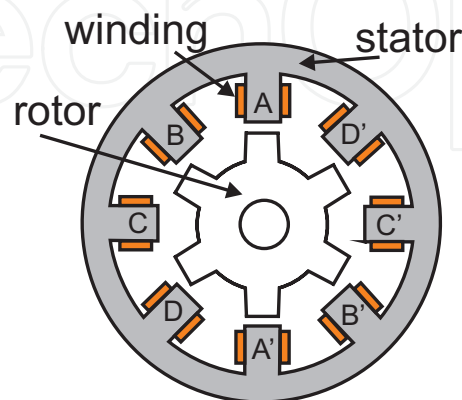

Figure 2. Front view of a switched reluctance machine 8/6.

4. The switched reluctance generator (SRG)

The switched reluctance generator (SRG) is an electromechanical energy converter capable of transforming mechanical energy into electrical energy. To operate as a generator, the machine must be excited during the degrowth of inductance and a mechanical torque must be applied on the machine shaft. The magnetization of the phase conjugate added to the input of the mechanical axis of the machine causes an emf appears which increases the rate of growth of the current curve [9, 21].

A typical drive system for switched reluctance generator is shown in Figure 3. This drive the SRG structure consists of a converter and a control system in closed loop since the SRG is unstable for operation in open loop [9]. The converter of Figure 3 drives the SRG and it is represented only one phase of SRG. Drive for a number of phase SRG higher is given below. The SRG can power the load directly as shown in Figure 3 or send energy to the grid using another power electronic converter.
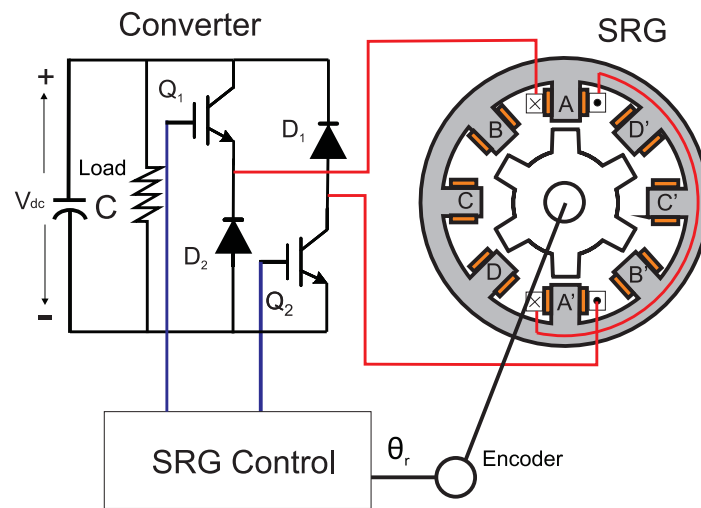

Figure 3. Drive system of SRG.

4.1. SRG converters

The SRG operates in two stages: excitation and generation. The excitation stage is performed when one phase of the SRG is submitted to the excitation voltage, which causes current flow in the winding of this growing phase (Figure (4)). In generating the current through the SRG phase to the load. In each period of the excitation voltage bus transfers energy to the magnetic field of the corresponding phase. In the generation period this energy flows to the load together with the share resulting from the conversion of mechanical energy into electrical [4, 20, 22]. Therefore, the SRG drive converter should be able to apply voltage in individual phases of the machine and create a path for the generated energy can flow to the electrical load.

There are several converters to drive the SRG, but the asymmetrical half-bridge converter AHB (Assimetric Half Bridge), Figure 5, is the most used because it allows robustness and the stages of regeneration energy and free-wheel when needed.

The converter of Figure 5 makes the SRG self excited, an initial excitation is required for the operation of the SRG. Usually the initial excitation is provided by an external source (a
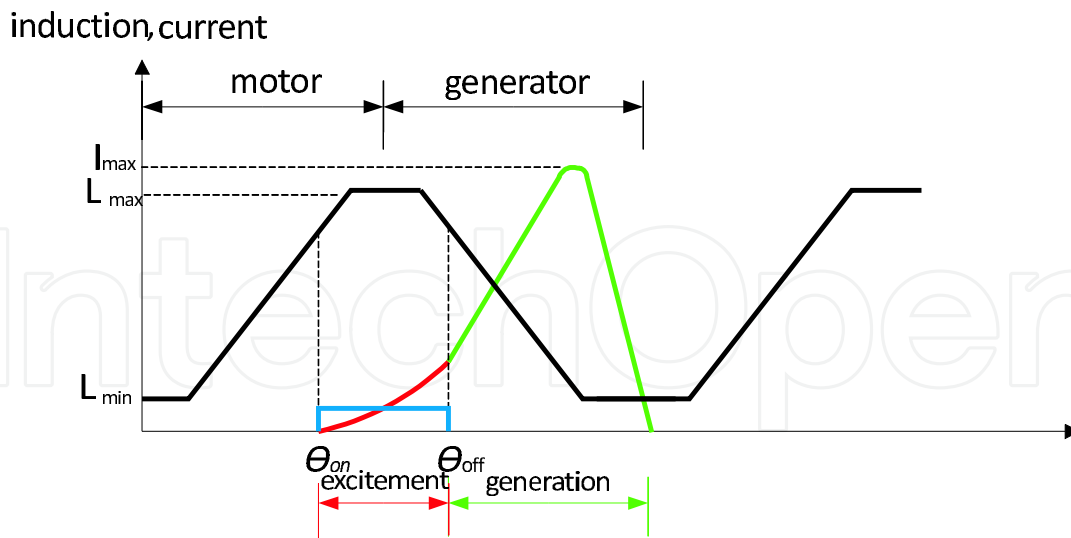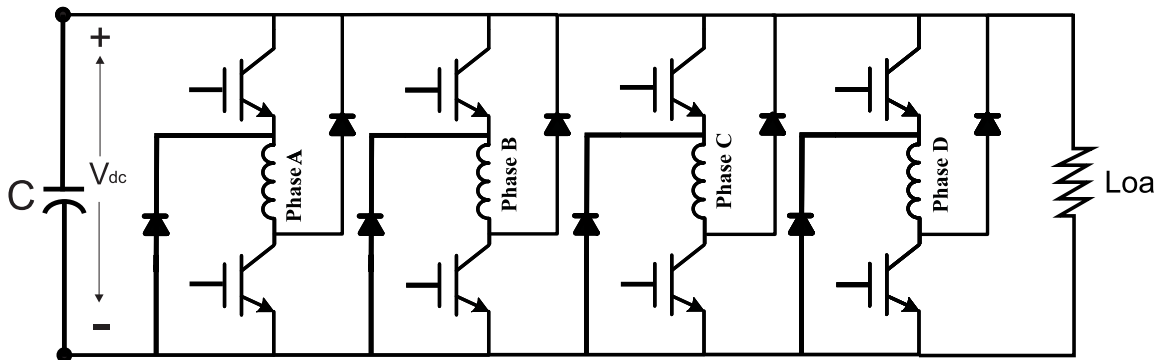
Figure 4. Profile of the Inductance..

Figure 5. Converter AHB four phase.

battery for example) until the capacitor is charged. This pass the same capacitor exciting the phases when the external source is removed. The capacitor also has the function of stabilizing the voltage delivered to the load.

The Figures 6(a) e 6(b) illustrates the stages of operation of the AHB converter. In the excitation stage (Figure 6(a)) the two switches (of phase to be excited) turn on. Then a current flows from the capacitor to the stage, magnetizing it. After the excitation interval both switches are opened and the diodes are now to conduct the generated energy to the load and recharge the capacitor (Figure 6(b)). This process is repeated cyclically for each phase of the converter.

One of the main advantages of this converter is its flexibility in the control individually of current in each phase. Furthermore the converter not allowing short circuit in DC bus converter due to the fact that the switches connected in series with machine winding [10, 23]. However, this configuration is not the cheapest, because it requires two semiconductor switches per phase of the SRG. There are topologies that use less than two switches per phase of the GRV, as shown in [10, 20, 24], but these topologies have limitations regarding the AHB converter as the literature describes.
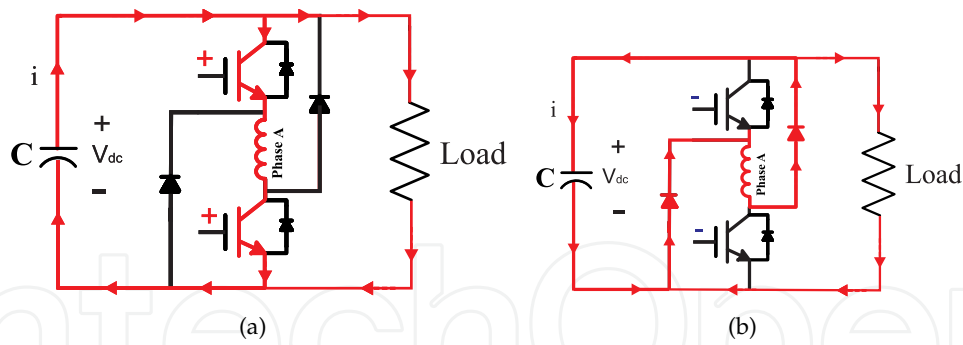
Figure 6. a) Excitation stage b) Generation stage.

4.2. SRG drive control

The SRG control is accomplished through the control of the switches of its converter. The SRG control requirements depending of each application. The quantities for controlling the generation of SRG is the period of excitement, the operating speed and excitation voltage [10]. When the load is connected directly to the converter (Figure 5) is necessary to provide a controlled voltage to the load. In case of load change control must act on the above quantities to maintain the generated voltage constant. This type of control is known as SRG voltage control bus. There are several controls proposed for this type of configuration as shown in [21]. This type of control is important for embedded applications such as vehicle and aerospace, where there is a need to maintain the dc bus voltage (responsible for food loads) at a constant value [10]. Figure 7 illustrates the typical configuration of this control.
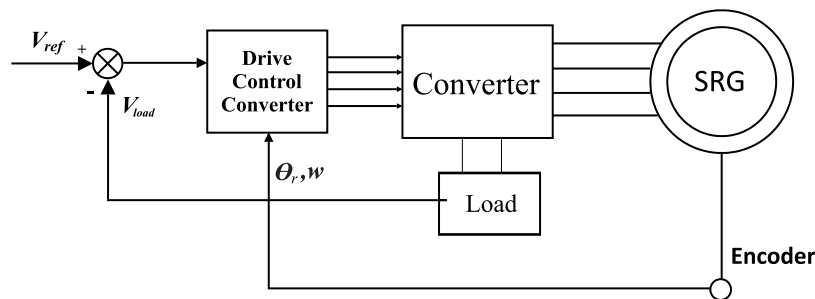

Figure 7. Bus voltage control structure.

When it is desired that the SRG operate at its optimum generation point is desirable controller the power generated directly [25, 26]. The typical control is shown in Figure 8. This control is typically used for power generation connected to the grid as seen in [25, 26]. The main applications of this type of control is in wind generation and generators driven by steam turbines . In this case the SRG is not connected directly with the load, but with another power converter that is responsible for sending the generated energy to the grid.

5. The power control system of the SRG

In this section its presents a technique of power control for the GRV connected to the grid. Unlike the controls proposed in [2, 4, 11] the converter connected to the generator is responsible for controlling the power to be generated and the other converter connected to the grid controls the voltage V_{dc} and its sends the energy generated to the grid.
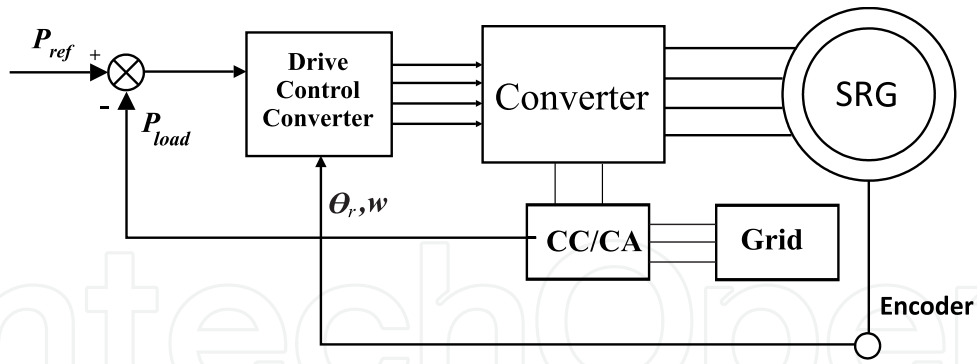
Figure 8. Generated power control structure.

5.1. Power converters

The converter used to drive the GRV was the AHB converter. This converter is connected via the DC link with the voltage source converter that it is connected to the grid.
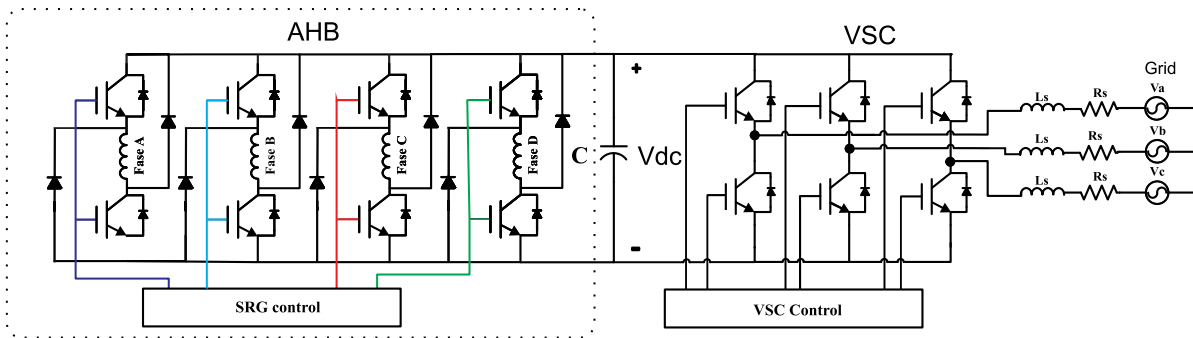

Figure 9. Power converters.

5.2. Direct Power Control

The direct power control system for SRG must regulate the power generated at the point of maximum aerodynamic efficiency, in other words, $P_{ref} = k_{opt}w_r^3$, where P_{ref} is the reference of active power. The proposed direct power control system consists in control the power generated by SRG directly. The diagram of the direct power control is shown in Figure 10. The control consists in keeping angle of activation of the switches of the HB converter at a fixed value θ_{on}. The PI controller processes the error (e_P) between P_{ref} and the generated power P and controls angle of shutdown of the switches θ_{off}, as shown in Equation (4). Thus, the principle of the control is when the step of the excitation increases, the generated power increases, as well.

The expression for the error power is given by:

$$e_P = P_{ref} - P \tag{3}$$

The angle θ_{off} is given by:

$$\theta_{off} = K_p e_P + K_i \int e_P dt \tag{4}$$

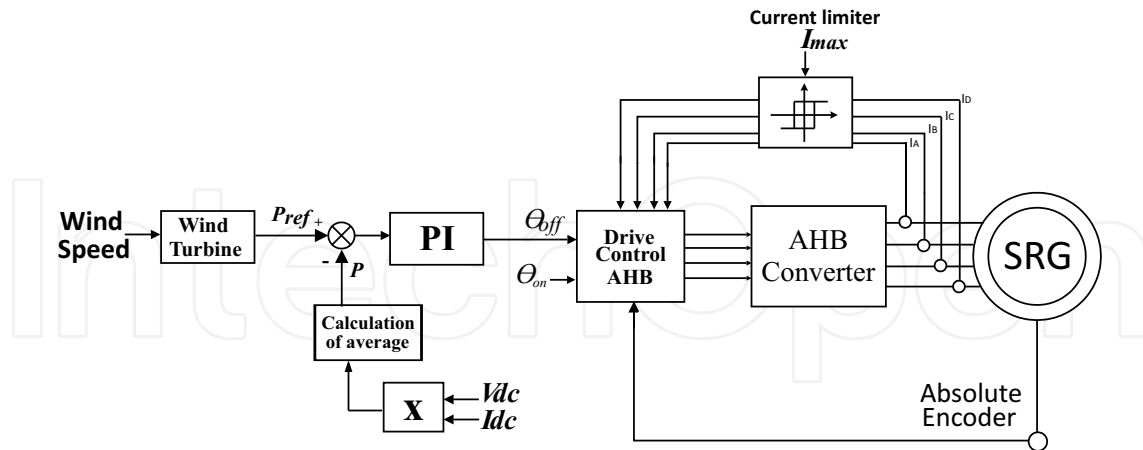where: K_p is the proportional gain and k_i is the integral gain of PI controller.

Figure 10. Diagram of direct power control for SRG.

5.2.1. Tuning of PI controller gains

The PI controller gains were adjusted using the second tuning method of Ziegler-Nicholds described in [27]. Figure 11 illustrates the procedure performed. Initially, the integral gain is zero and sets the proportional gain value (K_p) for the closed loop system, until the point where the response of the system starts to oscillate periodically. This setpoint is known as the critical point, in which the period of oscillation is defined as the critical period (P_{cr}) proportional gain and proportional gain is defined as critical (K_{cr}). From the P_{cr} e K_{cr} PI controller gains are determined using the relationship shown in Equation 5. This technique allows a good initial value of line when you do not know the process of plant be controlled.

$$K_p = 0.45 K_{cr}$$
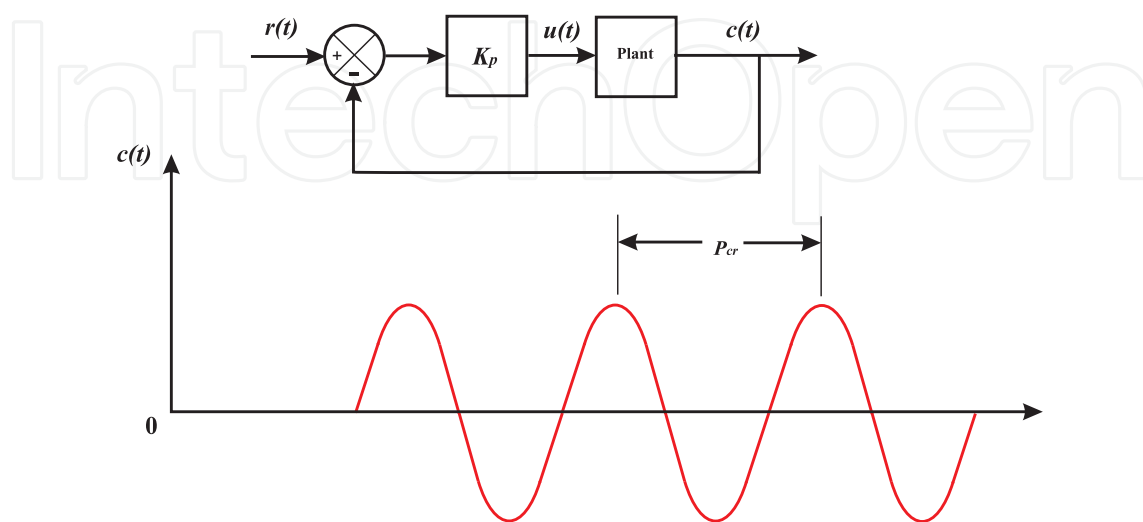$$K_i = \frac{1}{2} P_{cr} K_{cr} \qquad (5)$$

Figure 11. Second tuning method of Ziegler-Nicholds.

5.3. Power Grid Connection Converter

The Voltage Source Converter (VSC), shown in Figure 9, controls the voltage V_{dc} and it allows to send the generated power by SRG to the grid. The control strategy applied to the converter voltage source consists of two control loops. There is an internal control loop that controls the current sent to the grid, and, externally, there is a control loop of bus voltage control (V_{dc}). The current loop control (i_{sd}, i_{sq}) is responsible for controlling the power factor of the power sent to the grid [28]. The control voltage of the DC link is responsible for balancing the flow of power between the SRG and the grid [29].

The DC link voltage control of the voltage source inverter is realized in the synchronous coordinate system (dq) with employment grid voltage angle ($\theta = wt$) used in the transformation $abc\ dq$, which is obtained using a Phase-Locked Loop (PLL). The control voltage of the DC link (V_{dc}) is performed by a PI controller, which comes from the reference value i_{sd}^* (6), while the value of i_{sq}^* is derived from the power factor desired FP and P_{ref} (7).

$$i_{sd}^* = K_{pi}(V_{dc}^* - V_{dc}) + K_{ii} \int (V_{dc}^* - V_{dc})dt \tag{6}$$

$$i_{sq}^* = \frac{-3}{2}\hat{P}_{ref}\frac{\sqrt{1-FP^2}}{FP^2} \tag{7}$$

The reference values of current are compared with the values obtained from electrical grid (i_{sd} e i_{sq}) and are processed by two PI controllers that generate the value of the space vector voltage of grid $\vec{v}_{dq}$ (8) and (9) in the synchronous coordinate system (Equation 10). This space vector is transformed for the coordinate system abc generating the signals voltage $v_{mod_{abc}}$(Equation 11) which are then generated using the PWM sinusoidal. The control system for VSC is shown in Figure 12.

$$v_{ds} = K_{ps}(i_{sd}^* - i_{sd}) + K_{is} \int (i_{sd}^* - i_{sd})dt \tag{8}$$

$$v_{qs} = K_{ps}(i_{sq}^* - i_{sq}) + K_{is} \int (i_{sq}^* - i_{sq})dt \tag{9}$$

$$\begin{bmatrix} i_d \\ i_q \end{bmatrix} = \frac{2}{3} \begin{bmatrix} cos\theta & sen\theta \\ -sen\theta & cos\theta \end{bmatrix} \begin{bmatrix} 1 & -\frac{1}{2} & -\frac{1}{2} \\ 0 & \frac{\sqrt{3}}{2} & -\frac{\sqrt{3}}{2} \end{bmatrix} \begin{bmatrix} i_a \\ i_b \\ i_c \end{bmatrix} \tag{10}$$

$$\begin{bmatrix} v_a^{mod} \\ v_b^{mod} \\ v_c^{mod} \end{bmatrix} = \begin{bmatrix} 1 & 0 \\ -\frac{1}{2} & \frac{\sqrt{3}}{2} \\ -\frac{1}{2} & -\frac{\sqrt{3}}{2} \end{bmatrix} \begin{bmatrix} cos\theta & -sen\theta \\ sen\theta & cos\theta \end{bmatrix} \begin{bmatrix} v_d^{mod} \\ v_q^{mod} \end{bmatrix} \tag{11}$$
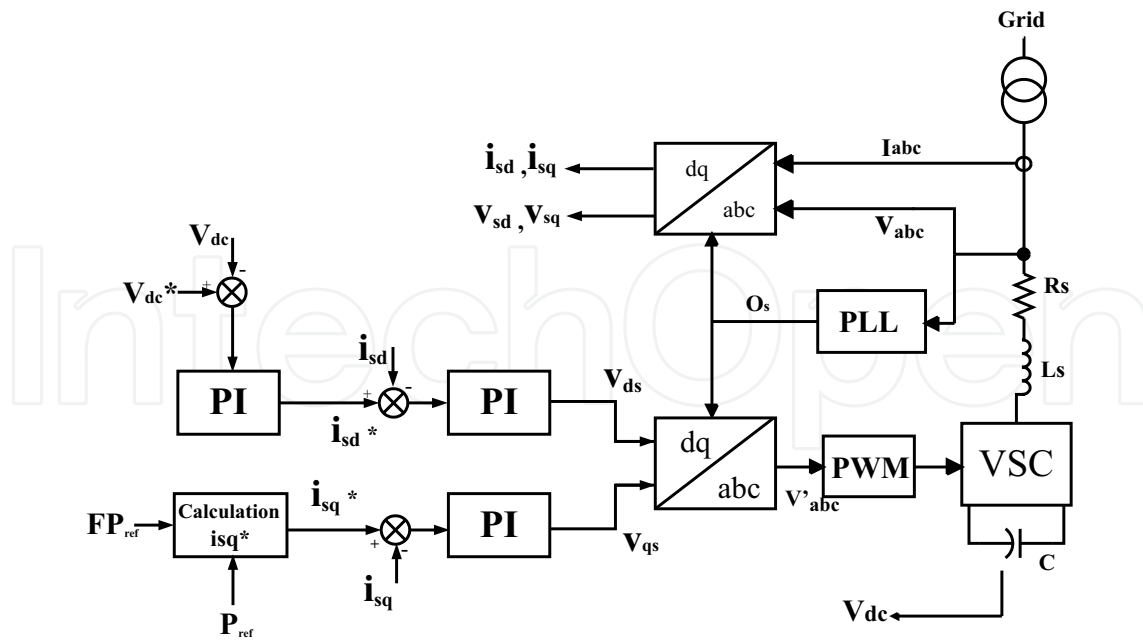
Figure 12. Block diagram of vector control of the converter connected to the grid.

5.4. PWM sinusoidal (SPWM)

There are several modulation techniques performed on the VSC to obtain a modulated voltage V_{abc}^{mod} in the terminals of the converter [30]. The most used technique is known as PWM sinusoidal (SPWM) using a triangular carrier for generating waveform desired [31].

SPWM modulation is obtained by comparing a reference voltage (sinusoidal) with a signal symmetrical triangular. The frequency of the triangular wave is to be at least 20 times greater than the maximum frequency of the reference signal, so that it is possible to obtain an acceptable reproduction of the waveform after filtering [32].
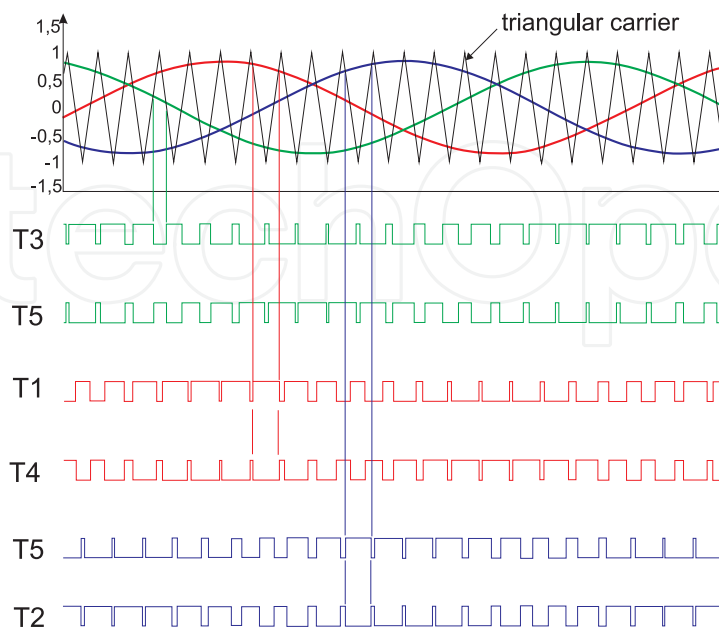

Figure 13. Modulation PWM sinusoidal

The Figures 13 shows the three-phase SPWM modulation signals used in this work. The carrier is compared with the reference sine wave for each phase, so that: when the carrier is greater than the reference phase, the switch top to respective phase is activated, otherwise the switch is operated below. Thus the output voltage of the modulated VSC is formed by a succession of rectangular wave. With a low pass filter can eliminate harmonic components generated by the modulation.

5.5. Synchronism with the grid

To perform the operations 10 e 11 correctly, it must obtain the angle of the voltages ($\theta = wt$). The main methods of obtaining the angle of the mains voltage are: method of zero crossing detection, filtering of the network voltages and PLL techniques. However, the use of a PLL is the most widely used technique due to its greater precision and less influence to the presence of harmonics and power grid disturbances in the grid [29].

There are various structures as described in [33]. However, the basic idea of operation of the PLL is to detect a difference between the instantaneous internal reference signal and external signal, as illustrated in Figure 14. The filter produces an error voltage proportional to the phase/frequency between the signals and operates in the VCO (Voltage Controlled Oscillator), which is a voltage controlled oscillator to change the frequency. So that internal matching the frequency of the signal external now obtains the angle of the external signal.
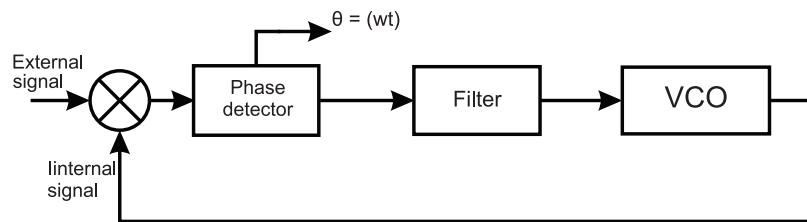

Figure 14. Basic idea of operation of the PLL.

The technique used in this work is known as three-phase SRF PPL (synchronous reference frame). This technique is the most widely used because it has little influence on the presence of harmonics and disturbances in the grid [34, 35].

Figure 15 shows the block diagram of three-phase PLL SRF. The basic operation of this PLL is to synchronize the synchronous reference frame PLL with the vector of the mains voltage.
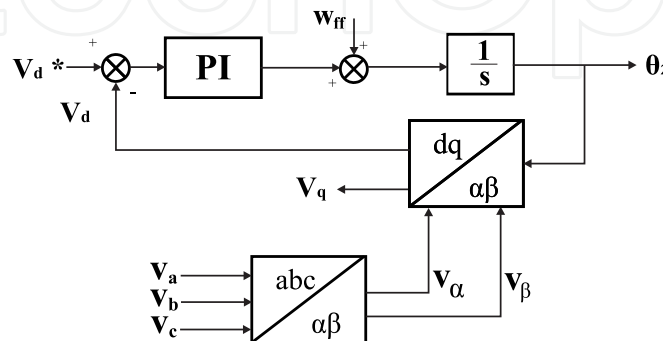

Figure 15. PPL synchronous reference frame

The voltages of the network (v_a, v_b, V_c) are obtained and then are transformed to stationary reference frame, using Equation 12. So has v_α e v_β using the proper angle estimated (θ_2), the variables v_α and v_β are transformed into the synchronous reference frame (Equation 13) resulting in tensionsv_d e v_q. Reference voltage v_d^* is set to zero. The error between v_d and v_d^* is processed by a PI controller that changes the value of (θ_2) in order to reset this error. When (θ_2) tends to the value of (θ_1) the sine tends to zero and the PLL is locked. In this situation, the value V_q is equal to the amplitude of the input voltages. The frequency obtained directly (w_{ff}) is added to improve the performance of the PLL.

$$\begin{bmatrix} v_\alpha \\ v_\beta \end{bmatrix} = \begin{bmatrix} 1 & -\frac{1}{2} & -\frac{1}{2} \\ 0 & \frac{\sqrt{3}}{2} & -\frac{\sqrt{3}}{2} \end{bmatrix} \begin{bmatrix} v_a(t) = V\cos(\theta_1) \\ v_b(t) = V\cos(\theta_1 - \frac{4\pi}{3}) \\ v_c(t) = V\cos(\theta_1 - \frac{2\pi}{3}) \end{bmatrix} = \begin{bmatrix} V\cos\theta_1 \\ -V\sin\theta_1 \end{bmatrix} \tag{12}$$

$$\begin{bmatrix} v_d \\ v_q \end{bmatrix} = \begin{bmatrix} \cos\theta & \sin\theta \\ -\sin\theta & \cos\theta \end{bmatrix} \begin{bmatrix} v_\alpha \\ v_\beta \end{bmatrix} = \begin{bmatrix} -V\sin(\theta_1 - \theta_2) \\ V\cos(\theta_1 - \theta_2) \end{bmatrix} \tag{13}$$

5.6. SRM nonlinear model

Below will be described the operation of the model proposed by [36] that was developed for simulation in Matlab-Simulink software. This model is based on of magnetization curve that can be obtained by experiments, calculated by finite element or determined analytically by means of machine parameters that are available. The inputs of this model are the stator voltages in the phases of the machine and the outputs are the mechanical variables (torque, speed and rotor position).

5.6.1. General configuration model

The general configuration of the nonlinear simulation model can be seen in Figure 16. This model can be divided into 3 parts: model circuit, calculating the electromechanical torque and mechanical model.

The data of the magnetization curves of the machine are used to calculate the necessary magnetic characteristics in the model of the electrical circuit and for calculating the torque of the electromechanical machine.

5.6.2. Modeling the electrical circuit

The electrical circuit of a SRM of F stages, consisting of a resistor in series with an inductance is not linear for each phase of the machine. It has been that the flow equation for a phase j of MRV is given by:

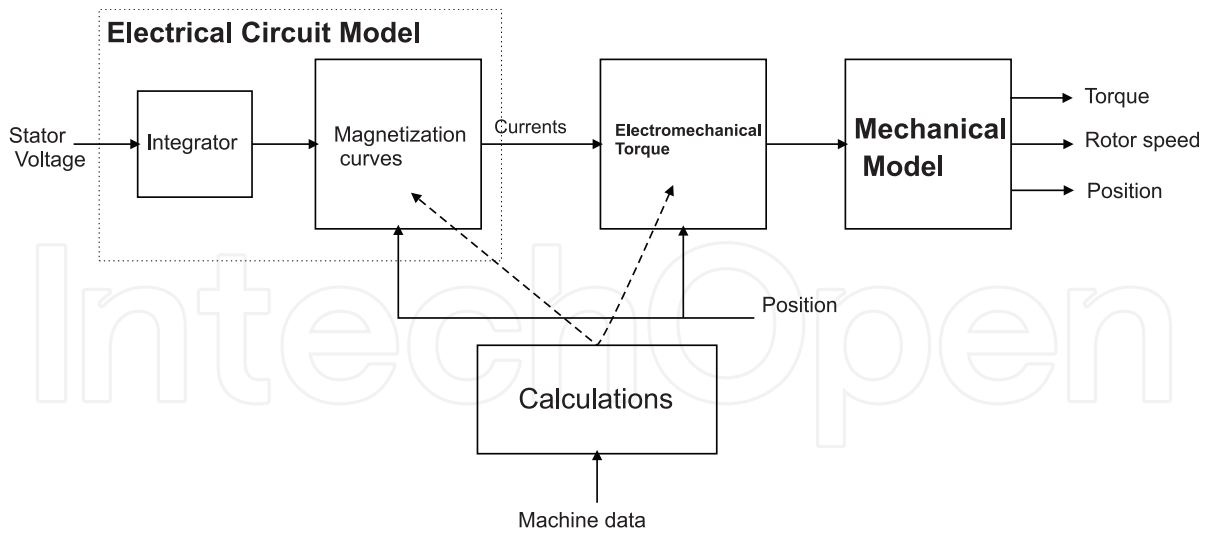$$\phi_j(t) = \int_0^t (V_j - R_j i_j) dt \tag{14}$$

Figure 16. General configuration of the nonlinear model.

The currents in the stator phases are nonlinear functions $I(\phi, \theta)$ tha can be calculated from the magnetization curves $\phi(I, \theta)$. Therefore the electric circuit of a phase of MRV is modeled as shown in Figure 17.
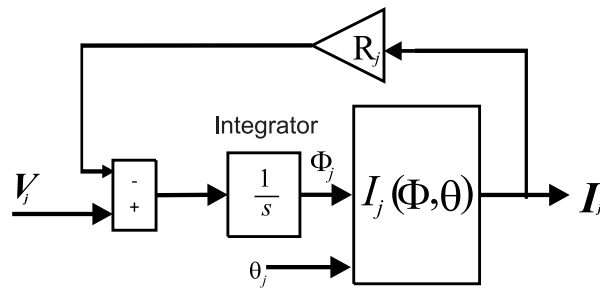

Figure 17. Electrical circuit model.

5.6.3. Magnetization curves.

The magnetization curves $\phi(I, \theta)$ are highly nonlinear due to the fact that MRV mainly operates in the saturation region. These curves can be obtained mainly in three ways: calculated by finite elements, analytical approach and experimental measurements.

5.6.4. Experimental measurements

The magnetization curves of MRV can be obtained through different forms as described in [37]. One way of measuring the magnetization curves are based on Equation 14. For each position of the rotor, a voltage is applied to the winding machine and the phase of the current and voltage are measured and stored. Then the magnetization curves are obtained from the processing of the waveforms of voltage and current. Figure 18 show the curves is observed in a test performed on an experimental MRV 8/6 obtained in [38].

This form of the curves is more accurate, but need experimental setup to perform measurements on the machine.
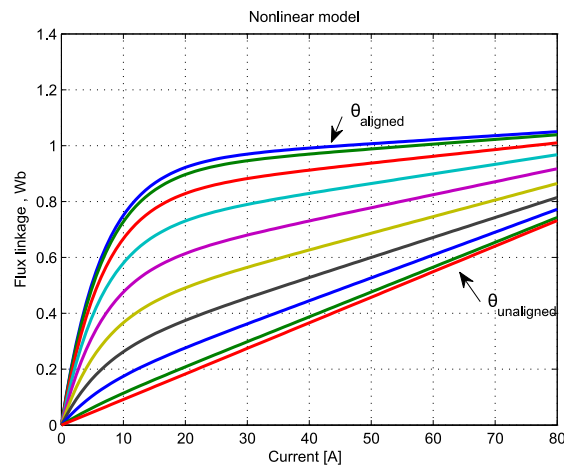
Figure 18. Experimental curver measurements.

5.6.5. Electromechanical torque

The electromechanical torque in SRM is the sum of the individual torques developed at each stage. When the magnetization curves are obtained experimentally or finite element electromechanical torque may be calculated using the equation of torque:

$$T_e = \frac{\delta W_f'}{\delta \theta} = \frac{\delta W_f'(i, \theta)}{\delta \theta} = \frac{dL(i, \theta)}{d\theta} \frac{i^2}{2} \tag{15}$$

Where (W_f') is the coenergy.

5.6.6. Mechanical model

The equation of the mechanical model is given by:

$$T_m = T_{emag} - Dw - J\frac{dw}{dt} \tag{16}$$

The mechanical model is then modeled as shown in Figure 19.
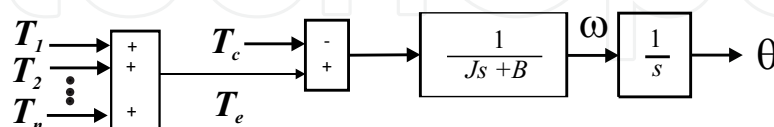

Figure 19. Mechanical model.

5.7. Machine model in Simulink

The nonlinear model developed by [36] became a block from the Simulink library SimPowerSystem. This block has an operating structure that can be viewed in Figure 20. From the data of magnetization of the two tables are created MRV. The table of current (ITBL) used in the model circuit and the torque table (TTBL) that gets the touch electromechanical

each phase. For input values that do not exist in the tables the outputs are obtained by linear interpolation. The total electromechanical torque is obtained by summing the phases torques and sent to the mechanical model. The rotor position is obtained by integrating the speed of the machine. The bold lines refer to multiple streams of data that depends on the number of phases of the machine. The currents obtained from the table of the currents are generated at the terminals of the machine model.
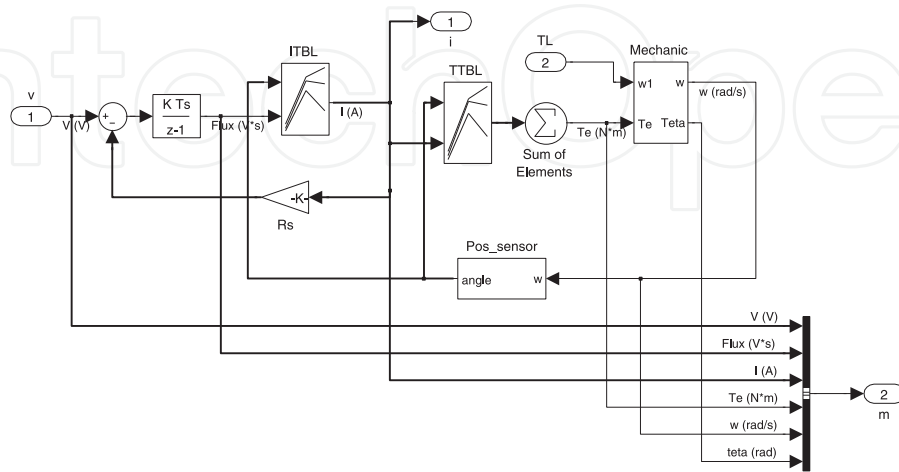

Figure 20. Diagram SRM model in Simulink.

6. Simulation results

The power control system proposed for the SRG connected to the grid was simulated using the Matlab-Simulink software . It was simulated a power profile (Figura 21) to be generated by the SRG in variable speed operation (Figura 23) and it observed that the reference active power was followed by the proposed DPC. In Figure 22 is observed the profile for the power factor of the energy sent to the grid and the output reach the reference..
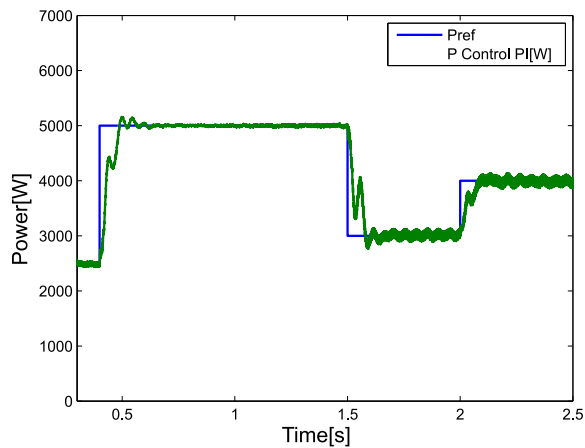

Figure 21. Power generated by SRG and the reference power.

Figure 24 shows the inverter phase currents of the SRG, it which observe the variation of current amplitudes, a fact that is justified due to the fact the controller changes θ_{off}. As can be seen in Figure 10. The voltage phases was set to 280 V and this should be the voltage of the link current which is controlled by the VSC.
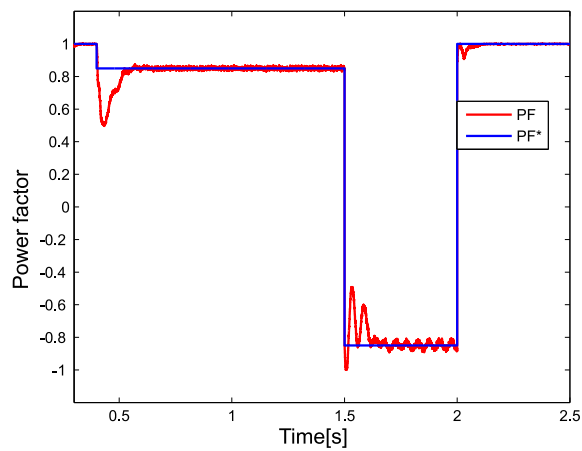
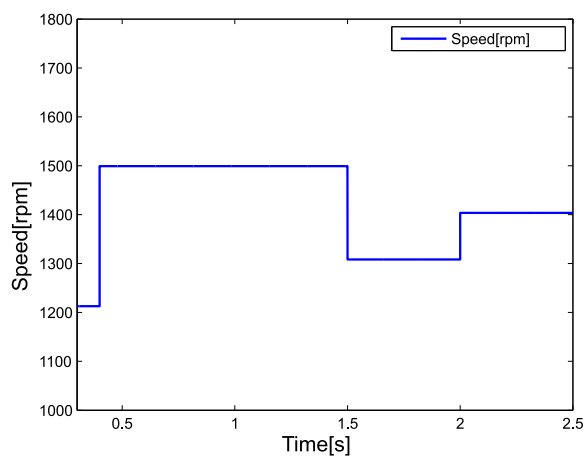**Figure 22.** Power factor of the energy sent to the grid.
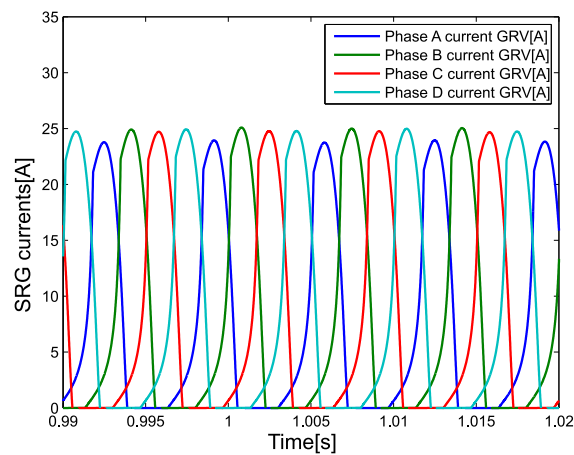

Figure 23. SRG operation speed.

Figure 24. SRG current phases.

Figures 25 and 26 presents V_{dc} voltage and the phase a voltage and current for the operation of the SRG and allow to observe the performance of the control performed on the converter.

In Figure 26 is observed the voltage and phase current from the power grid. The THD (Total Harmonic Distortion) of the current sent to the grid analyzed by FFT (emph Fast Fourier Transform) (Figure 27) was 1.57%.
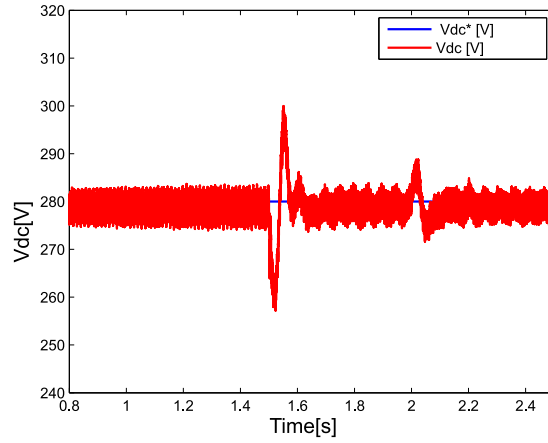

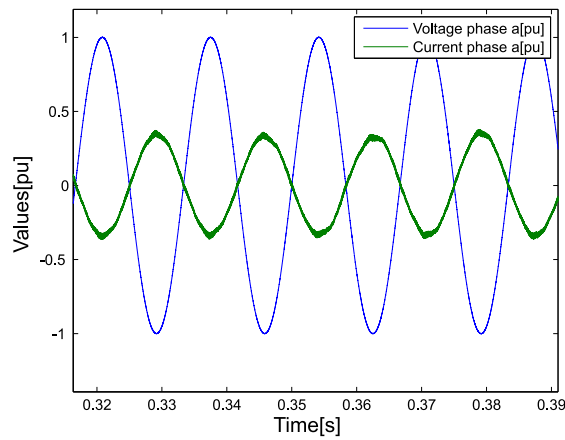**Figure 25.** Voltage V_{dc} controlled by VSC.

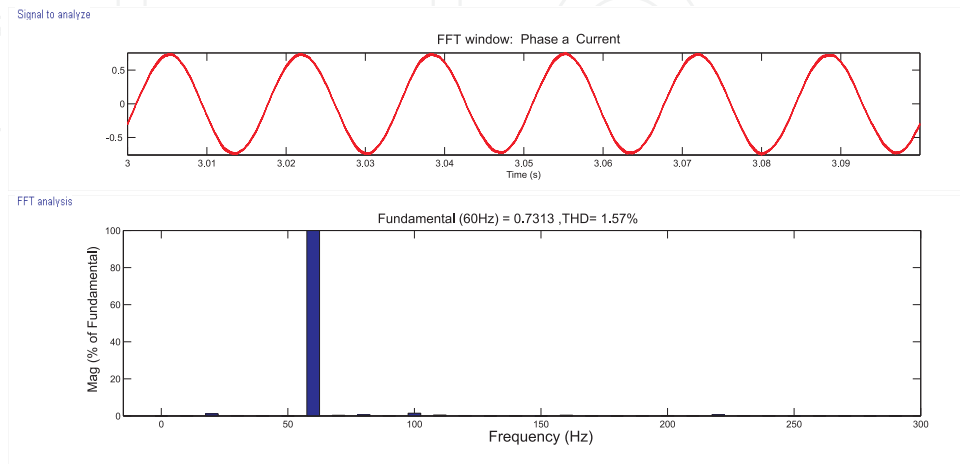**Figure 26.** Phase a voltage and current grid.

Figure 27. THD and harmonic components of the phase current.

7. Conclusions

This book chapter was presented a proposal for direct control of power for a SRG. The DPC controller allows the power control of the generator directly without using current loops. The controller has a satisfactory performance and no complexity for its implementation. The AHB converter allows robustness and the stages of regeneration energy and freewheel when needed. The simulation results confirm the effectiveness of the power controller during conditions of generator operation at variable speed and with different reference values of active power and power factor. Thus, the strategy of direct control of power is an interesting tool to control the power of the variable reluctance generator powered wind turbines.

Acknowledgements

Author details

Tárcio A. dos S. Barros[1,*],
Alfeu J. Sguarezi Filho[2] and Ernesto Ruppert Filho[1]

* Address all correspondence to: tarcio@dsce.fee.unicamp.br

1 Universidade Estadual de Campinas-UNICAMP, Faculdade de Engenharia Elétrica e Computação-FEEC, DSCE, Campinas, Brazil
2 Universidade Federal do ABC-UFABC, Santo André, Brazil

References

[1] Association World Wind Energy. *The World Wind Energy 2011 report*, 2012.

[2] McSwiggan D., L. Xu, and T Littler. Modelling and control of a variable-speed switched reluctance generator based wind turbine. *Universities Power Engineering Conference*, pages 459 – 463, June 2007.

[3] K. Ogawa, N. Yamamura, and M. Ishda. Study for small size wind power generating system using switched reluctance generator. *IEEE International Conference on Industrial Technology*, pages 1510–1515, 2006.

[4] R. Cardenas, R. Pena, M. Perez, G. Claro, J. Asher, and P. Wheeler. Control of a switched reluctance generator for variable-speed wind energy applications. *IEEE Transactions on energy conversrion*, 20(4):691 –703, December 2005.

[5] Alfeu J. Sguarezi Filho. Controle de potências ativa e reativa de geradores de indução trifásicos de rotor bobinado para aplicação em geração eólica com a utilização de controladores baseados no modelo matemático dinâmico do gerador. Tese doutorado, Faculdade de Engenharia Elétrica e Computação, Unicamp - Universidade Estadual de Campinas, Novembro 2010.

[6] Y. He, J. Hu, and Z. Rend. Modelling and control of wind-turbine used dfig under network fault condition. *Proceedings of the Eighth International Conf. on Electrical Machines and Systems*, 2:096–991, September. 2008.

[7] Seul-Ki Kim and Eung Kim. Pscad/emtdc-based modeling and analysis of a gearless variable speed wind turbine. *IEEE Transactions on energy conversrion*, 22(2):096–991, June 2007.

[8] Y. Chang and M. Liaw. Establisment of a switched reluctance generator-based common dc microgrid system. *IEEE transactions on power electronics*, pages 2512–2526, September. 2011.

[9] D.A. Torrey. Switched reluctance generators and their control. *Industrial Electronics, IEEE Transactions on*, 49(1):3 –14, feb 2002.

[10] T. Sawata. *The switched reluctance generator, Electronic Control of Switched Reluctance Machines*. Newness Power Engineering Series, 2001.

[11] S.F. Azongha, S. Balathandayuthapani, C.S. Edrington, and J.P. Leonard. Grid integration studies of a switched reluctance generator for future hardware-in-the-loop experiments. *Universities Power Engineering Conference*, pages 459 – 463, June 2010.

[12] Zhenguo Li, Jian Ma, Chunjiang Zhang, Dong-Hee Lee, and Jin-Woo Ahn. Research of switched reluctance wind power generator system based on variable generation voltage converter. In *Electrical Machines and Systems (ICEMS), 2010 International Conference on*, pages 418 –421, oct. 2010.

[13] H. Chen. Implementation of a three-phase switched reluctance generator system for wind power application. *IEEE International Conference on Industrial Technology*, (8):1 –6, June 2008.

[14] Baiming ShaD and Ali Emadi. A digital control for switched reluctance generators. *IEEE International Conference Mechatronics*, (4):182 –187, April 2000.

[15] Yilmaz Sozer and David A. Torrey. Closed loop control of excitation parameters for high speed switched-reluctance generators. *IEEE International Conference on Industrial Technology*, (4):1 –6, June 2000.

[16] K. Iordanis and C. Mademlis. Optimal efficiency control of switched reluctance generators. *IEEE Transactions on power electronics*, 21(4):1062–1071, April 2006.

[17] M. Godoy Simões and Felix A. Farret. *Renewable Energy Systems with Induction Generators*. CRC PRESS, 2004.

[18] Maurício B. C. Salles. Modelagem e análises de geradores eólicos de velocidade variável conectados em sistemas de energia elétrica. Tese doutorado, Escola Politécnica da Universidade de São Paulo, 2009.

[19] Manfred Stiebler. *Wind Energy Systems for Electric Power Generation*. Springer, 2008.

[20] R. Krishnan. *Switched Reluctance Motor Drives,Modeling, Simulation, Analysis, Design, and Applications*. CRC PRESS, 2001.

[21] Augusto Wohlgemuth Fleury Veloso da Silveira. Controle de tensão na carga para motor/gerador a relutância variável de três fases. Tese, Faculdade de Engenharia Elétrica, UFU, Universidade Federal de Uberlândia, Fevereiro 2011.

[22] E.A.E. Jebaseeli and D. Susitra. Performance analysis of various configurations of switched reluctance machine for wind energy applications. In *Recent Advances in Space Technology Services and Climate Change (RSTSCC), 2010*, pages 419 –423, nov. 2010.

[23] Gang Yang, Zhiquan Deng, Xin Cao, and Xiaolin Wang. Optimal winding arrangements of a bearingless switched reluctance motor. *Power Electronics, IEEE Transactions on*, 23(6):3056 –3066, nov. 2008.

[24] A. Takahashi, H. Goto, K. Nakamura, T. Watanabe, and O. Ichinokura. Characteristics of 8/6 switched reluctance generator excited by suppression resistor converter. *Magnetics, IEEE Transactions on*, 42(10):3458 –3460, oct. 2006.

[25] S.M. Muyeen. *Wind Energy Conversion Systems: Technology and Trends*. Green Energy and Technology. Springer, 2012.

[26] R. Cardenas, R. Pena, M.Perez, G. Asher, J. Clare, and P.Wheeler. Control system for grid generation of a switched reluctance generator driven by a variable speed wind turbine. *30th IEEE Industrial Electronics Society Conference*, pages 2–6, June 2004.

[27] K. Ogata. *Engenharia de Controle Moderno*. LTC, 2000.

[28] M. Kazmierkowski and L. Malesani. Current control techniques for three-phase voltage-source pwm converters: a survey. *Industrial Electronics, IEEE Transactions on Industrial Electronics*, 45(5):691 –703, October 1998.

[29] Marco Liserre Adrian V. Timbus Frede Blaabjerg, Remus Teodorescu. Overview of control and grid synchonization for distributed power generation systems. *IEEE Transactions on industrial electronics*, 53(5):691 –703, October 2008.

[30] M.A. Boost and P.D. Ziogas. State-of-the-art carrier pwm techniques: a critical evaluation. *Industry Applications, IEEE Transactions on*, 24(2):271 –280, mar/apr 1988.

[31] José R. Rodríguez, Juan W. Dixon, José R. Espinoza, Jorge Pontt, and Pablo Lezana. Pwm regenerative rectifiers: State of the art. *IEEE Transactions on Industrial Electronics*, 52(1), February 2005.

[32] José Antenor Polímio. *Eletrônica de potência para geração,transmissão e distribuição de energia*, 2012.

[33] R. M. Santos Filho, P. F. Seixas, P. C. Cortizo, L. A. B. Torres, and A. F. Souza. Comparison of three single-phase pll algorithms for ups applications. *Industrial Electronics, IEEE Transactions on*, 55(8):2923 –2932, aug. 2008.

[34] F. Liccardo, P. Marino, and G. Raimondo. Robust and fast three-phase pll tracking system. *Industrial Electronics, IEEE Transactions on*, 58(1):221 –231, jan. 2011.

[35] D. Jovcic. Phase locked loop system for facts. *Power Systems, IEEE Transactions on*, 18(3):1116 – 1124, aug. 2003.

[36] H. Le-Huy and P. Brunelle. A versatile nonlinear switched reluctance motor model in simulink using realistic and analytical magnetization characteristics. In *Industrial Electronics Society, 2005. IECON 2005. 31st Annual Conference of IEEE*, page 6 pp., nov. 2005.

[37] Wen Ding and Deliang Liang. A fast analytical model for an integrated switched reluctance starter/generator. *Energy Conversion, IEEE Transactions on*, 25(4):948 –956, dec. 2010.

[38] T.J.E. Miller and M. McGilp. Nonlinear theory of the switched reluctance motor for rapid computer-aided design. *Electric Power Applications, IEE Proceedings B*, 137(6):337 –347, nov 1990.